Large $B(M1)$ Staggering at High Spins in ^{86}Zr: Broken Boson Pairs in the Four-Quasiparticle Regime

P. Chowdhury,[(1)] C. J. Lister,[(1)] D. Vretenar,[(1),(a)] Ch. Winter,[(1)] V. P. Janzen,[(2),(3)] H. R. Andrews,[(2)] D. J. Blumenthal,[(1)] B. Crowell,[(1)] T. Drake,[(4)] P. J. Ennis,[(1)] A. Galindo-Uribarri,[(4)] D. Horn,[(2)] J. K. Johansson,[(3)] A. Omar,[(3)] S. Pilotte,[(5),(b)] D. Prévost,[(3)] D. Radford,[(2)] J. C. Waddington,[(3)] and D. Ward[(2)]

[(1)]*A. W. Wright Nuclear Structure Laboratory, Yale University, New Haven, Connecticut 06511*
[(2)]*Atomic Energy of Canada Limited Research, Chalk River Laboratories, Chalk River, Ontario, Canada K0J 1J0*
[(3)]*Tandem Accelerator Laboratory, McMaster University, Hamilton, Ontario, Canada L8S 4K1*
[(4)]*University of Toronto, Toronto, Ontario, Canada M5S 1A7*
[(5)]*Laboratoire de Physique Nucléaire, Université de Montréal, Montréal, Québec, Canada H3C 3J7*
(Received 12 August 1991)

The transitional nucleus ^{86}Zr has been studied by the ^{60}Ni(^{30}Si,$2p2n$) reaction, with γ-γ coincidence, angular correlation, and Doppler-shift-attenuation measurements. Band structures exhibiting strongly staggered $M1$ transition rates were found at high spins, with large $B(M1)$ values but no significant $E2$ collectivity. The unusual behavior of this nucleus is interpreted within the framework of an interacting boson model incorporating two broken boson pairs. This new model for high-spin states is seen to be remarkably successful in describing the electromagnetic decay properties in the four-quasiparticle regime.

PACS numbers: 23.20.−g, 21.60.Fw, 27.50.+e

The recent refinement of cranked shell models has allowed considerable advances in our understanding of deformed nuclei, especially in the rotational evolution of the shape of the most bound mean field, and the physics of shape coexistence and superdeformation. The range of applicability of the spherical shell model has also continued to expand and encompass increasing numbers of valence particles in larger model spaces, which permit more refined calculations of nuclear eigenstates and the transition matrix elements between them. However, in nuclei which have too few valence particles to assume permanent deformation, yet which lie too far from shell closures to allow spherical shell-model calculations, neither approach has been very successful. The deformed models neglect residual interactions, while the shell-model calculations require unrealistic truncation of the model space. The best insight into the behavior of these transitional nuclei has come from the interacting boson model (IBM) which can describe the evolution from sphericity to deformation, but until recently has been restricted to states of relatively low angular momentum. In this Letter we report a detailed experimental study of a transitional nucleus, ^{86}Zr, which is seen to exhibit striking features in its high-spin decay pattern. We also present an interpretation of its level structure up to high spins using a new extension of the IBM which incorporates up to two broken boson pairs to generate angular momentum.

Medium-mass nuclei with $80 < A < 90$ provide stringent tests for all nuclear models, as single-particle and collective degrees of freedom are excited at similar energies, and the structure of nuclei changes extremely rapidly with neutron and proton number. The neutron-deficient zirconium ($Z=40$) isotopes with $40 \leq N \leq 50$ provide a good example of such rapid changes. The $N=Z$ nucleus ^{80}Zr is one of the most deformed nuclei known [1] (polarized by a deformed shell gap at particle number 38), and has a low-lying rotational $J=2$ state at 289 keV. In contrast, the nucleus ^{90}Zr is spherical [2], with a neutron shell closure at $N=50$, and has a single-particle $J=2$ state at 2186 keV. The nucleus ^{86}Zr, with a $J=2$ state at 752 keV, lies at the transition between spherical and deformed nuclei, as highlighted by the level structures of its neighboring even-even isotopes. While ^{84}Zr exhibits regular, stretched rotational cascades of enhanced $E2$ transitions [3] which are characteristic of deformed nuclei, ^{88}Zr has a complex, irregular series of states with almost no collective enhancement, and can be understood in detail within the spherical shell model [2]. Several experiments had previously been performed on ^{86}Zr, and a variety of approaches used to interpret the data [4,5]. In this Letter we will concentrate on our new experimental data at higher spin and their interpretation.

The nucleus ^{86}Zr was studied in two separate experiments by the ^{60}Ni(^{30}Si,$2p2n$)^{86}Zr reaction, with a 135-MeV ^{30}Si beam from the Tandem Accelerator Superconducting Cyclotron (TASCC) facility at Chalk River. The first used two stacked 480-μg cm^{-2} self-supporting ^{60}Ni targets for minimizing the Doppler broadening of line shapes, in order to deduce the high-spin part of the level scheme. The aim of the second experiment was to measure the lifetimes of the high-spin states via the Doppler-shift-attenuation method (DSAM), and a 500-μg cm^{-2} ^{60}Ni target evaporated onto a 12.5-mg cm^{-2} Au backing was used. Gamma rays were detected with the 8π spectrometer. The level scheme was constructed from a γ-γ matrix which optimized the relative yield of the $2p2n$ evaporation channel by filtering events where, in addition to at least 2 out of 20 Compton-suppressed Ge detectors, at least 14 out of 71 elements of the BGO multiplicity array had fired. For the angular correlation analysis, the stacked-target γ-γ data were sorted according to the polar angle of the Ge detectors with respect to the beam direction, and directional correlation intensity ratios were extracted. For the DSAM analysis, the backed-target data were sorted into two γ-γ matrices, tagged according to whether the γ rays were detected in the forward (37°) or backward (143°) ring of five detectors. Both upstream and downstream data sets were analyzed to check for systematic errors. Line shapes were fitted with the program GNOMON [6], which corrects for geometric, relativistic, and layered-target effects, as well as those due to complex feeding patterns.

Figure 1 shows a partial level scheme of ^{86}Zr deduced from the present work. States have been identified up to an excitation energy of ~14 MeV, which is about twice that observed in previous work [5]. Spin and parity assignments are based on the angular correlation analysis and lifetime information. In addition to the yrast cascade, which has been established to $J^\pi = 24^+$, non-yrast structures have been extended considerably. Except for revised spin assignments for the top two states observed in the earlier work [5], the previously published level scheme is corroborated. The results of the DSAM line-shape analysis for the high-spin states are summarized in Table I. Best fits to the line shapes were obtained with continuum feeding times between 120 and 180 fs; however, the unobserved feeding was not well determined, and the errors on the measured lifetimes include this systematic uncertainty. The experimentally determined branching ratios of the transitions in this cascade and the fitted multipole mixing ratios allowed the extraction of absolute $B(E2)$ and $B(M1)$ rates, which are also given in Table I.

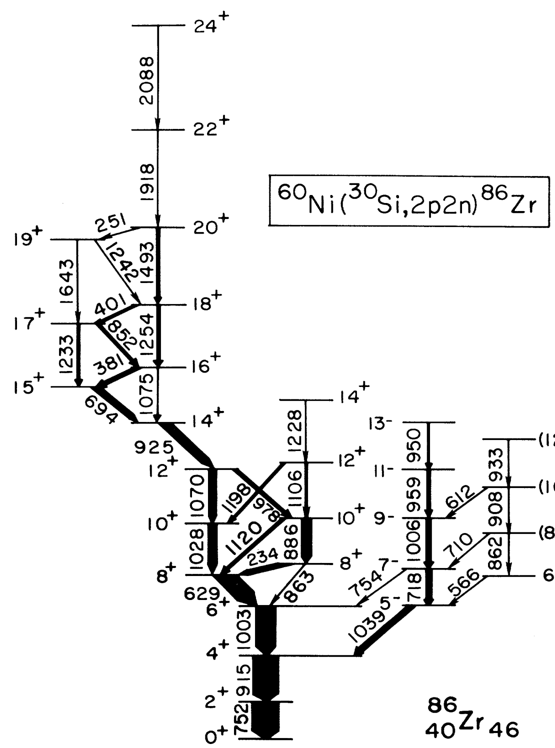

FIG. 1. Partial level scheme of ^{86}Zr deduced in the present work. Transition energies are in keV.

TABLE I. Lifetimes and transition rates within the high-spin yrast cascade in ^{86}Zr. The asymmetry of errors on the lifetimes include systematic uncertainties in the sidefeeding times (see text). [For $E2$ transitions, 1 Weisskopf unit (W.u.) = 2.3 $\times 10^{-3}\, e^2 b^2$; for $M1$ transitions, 1 W.u. = $1.8\mu_N^2$.]

J_i^π	τ (fs)	$E_\gamma(E2)$ (keV)	$E_\gamma(M1)$ (keV)	$B(E2)$ (W.u.)	$B(M1)$ (μ_N^2)
15^+	800^{+200}_{-30}	...	694	...	$0.21^{+0.01}_{-0.04}$
16^+	850^{+200}_{-30}	1075	381	$7.8^{+0.6}_{-1.8}$	$0.88^{+0.05}_{-0.18}$
17^+	220^{+150}_{-30}	1233	852	$18.0^{+3.8}_{-7.8}$	$0.28^{+0.05}_{-0.12}$
18^+	330^{+70}_{-30}	1254	401	$16.8^{+2.2}_{-3.3}$	$1.38^{+0.18}_{-0.27}$
19^+	100^{+120}_{-30}	1643	1242	$19.1^{+9.3}_{-10.8}$	$0.11^{+0.06}_{-0.06}$
20^+	400^{+120}_{-50}	1493	251	$10.2^{+1.5}_{-2.5}$	$1.45^{+0.30}_{-0.40}$
22^+	80^{+100}_{-50}	1918	...	$17.4^{+28.9}_{-9.7}$	...
24^+	90^{+120}_{-60}	2088	...	$10.1^{+20.2}_{-5.8}$	...

Our discussion will focus on the new positive-parity yrast sequence which extends from spin $J = 14$ to 24. The lifetimes and transition rates of states below $J = 14$ in ^{86}Zr had been measured previously [5,7], with the largest $E2$ matrix element being the $2^+ \to 0^+$ decay of 14 ± 3 Weisskopf units (W.u.). The pattern of $E2$ decays at low spins is inconsistent with either simple rotational or simple vibrational behavior, as the $B(E2)$ values decrease with spin. The level spacings of the states above $J = 14$ resemble the rotational cascades characteristic of deformed nuclei, where the staggering in energy of the odd and even spins would be interpreted as the signature splitting often associated with nonaxial shapes. Thus, it appears plausible that the nucleus has undergone a shape change and rotational motion has become the energetically favored mode of carrying angular momentum. Such a change should, therefore, be clearly reflected in the transition matrix elements, particularly those of the $E2$ decays. However, inspection of Table I reveals that, in the high-spin regime studied in the present work, the $B(E2)$ values show no enhancement relative to the low-spin states, and remain between 10 and 20 W.u. For rotational excitations of an axially deformed nucleus, this would imply a deformation of $\beta_2 \sim 0.1$.

In sharp contrast to the rather constant behavior of the $E2$ decays, the $M1$ transition rates show an alternating pattern of low and extremely high ($\sim 1\mu_N^2$) values, as shown in Fig. 2. This is substantially larger than the average experimentally observed $B(M1)$ value of $\sim 0.05\mu_N^2$ for the $45 < A < 90$ region [8]. Although enhanced $M1$ transitions have been observed and described in both spherical [2] and deformed nuclei [9] in this mass

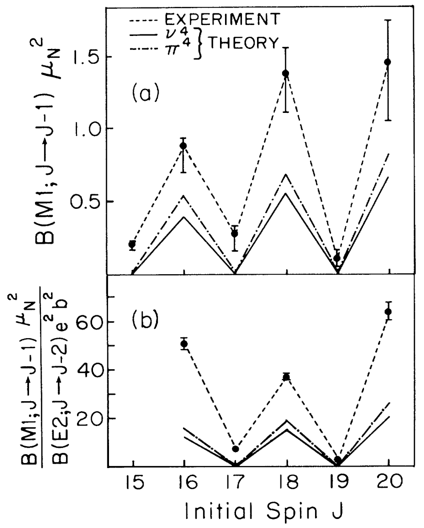

FIG. 2. Comparison of measured electromagnetic transition rates within the high-spin yrast cascade in ^{86}Zr (dashed lines) with model calculations for the $(N-2)\otimes(\nu g_{9/2})^4$ (solid lines) and $(N-2)\otimes(\pi g_{9/2})^4$ (dot-dashed lines) configurations.

region, the combination of the strong staggering of $B(M1)$ rates with spin, the large average $B(M1)$ values, and the weakly collective $B(E2)$ rates found in ^{86}Zr are difficult to explain in conventional models. In the cranking formalism, it is necessary to assume both a well-defined, fixed deformation at high spins and an unusual quasiparticle configuration in order to reproduce the $B(M1)$ staggering [10]. Given that the measured $B(E2)$ transition rates are quite low, it is not at all clear that such a description for ^{86}Zr is appropriate. In the spherical shell model approach, a strong truncation of the configuration space is required and only schematic results can be obtained. The distinctive pattern of the $B(M1)$ values in this transitional nucleus suggests an underlying symmetry in the structure of these states. To probe this underlying symmetry, we have used a recent extension of the IBM, which addresses the physics of high spins in transitional nuclei in terms of broken boson pairs [11,12].

The model is based on the IBM-1 [13], in which fermions couple pairwise to form s and d bosons, and no distinction is made between protons and neutrons. A recent extension of this model allows the breaking of one or two bosons to form noncollective fermion pairs, represented by two- and four-quasiparticle (qp) states, respectively, which can couple to their respective boson cores. The Hamiltonian has four terms: a bosonic part, a fermionic part, a boson-fermion interaction, and a pair-breaking interaction that mixes 0qp, 2qp, and 4qp configurations. The form and strength of most of these interactions are well established. All the parameters except the quasiparticle mixing were constrained by analyses of low-spin states of neighboring nuclei, and only the mixing term was adjusted to fit the data. A $Z=50$, $N=50$ core was used, resulting in a model space of $N=7$ bosons for ^{86}Zr, with $\varepsilon=0.74$ MeV for the single-boson energy, and $c_0=0.6$, $c_2=-0.23$, $c_4=0.12$, $v_0=-0.2$, and $v_2=0.14$ (all in MeV) for the boson-boson interaction parameters. This corresponds to a slightly anharmonic, near-vibrational core. For the noncollective fermionic part, it is not clear whether a pair of $g_{9/2}$ neutrons or a pair of $g_{9/2}$ protons aligns first, since the g factor of the first 8^+ state is not measured. Furthermore, from Fig. 1, it is seen that, slightly above the yrast 2qp excitations built on the 8_1^+ state, there is an almost identical structure built on the 8_2^+ state. It is very likely that one of these has a $(N-1)\otimes(\nu g_{9/2})^2$ and the other a $(N-1)\otimes(\pi g_{9/2})^2$ configuration. In the isotone ^{84}Sr, which also has two closely spaced 8^+ states, the measured g factors show that the neutrons align first [14]. We have assumed that the 2qp yrast structure in ^{86}Zr is based on the $(N-1)\otimes(\nu g_{9/2})^2$ configuration, and have performed detailed calculations of level spectra for neutron bands. A separate calculation is required in order to describe the structure of proton bands. A preliminary calculation in the restricted space of 0qp and 2qp showed that only the $\nu g_{9/2}$ orbital is important for near-yrast positive-parity states. The $\nu g_{9/2}$ single-quasiparticle energy was chosen to be 1.6 MeV to reproduce the excitation energy of the 8_1^+ state. Occupation probabilities were obtained in a standard BCS calculation with a pairing strength $G=24/A$ and Kisslinger-Sorensen [15] single-particle energies. The interaction between fermions was taken as a surface-delta interaction of strength $V_0=-0.5$ MeV. The boson-fermion coupling parameters were $\Gamma_0=0.3$ MeV for the strength of the dynamical interaction, $\chi=-1.0$ and $\Lambda_0=0.5$ MeV for the strength of the exchange interaction; the monopole interaction was neglected. Finally, for the mixing term, the strength parameters were $u_0=-1.5$ MeV and $u_2=-0.1$ MeV. The calculations describe the main features of the decay scheme remarkably well, including 2qp configurations of both positive and negative parity (with the $p_{1/2}$ orbital included in the fermion model space for negative parity states). A longer paper discussing all aspects of the calculation and comparison with data is in preparation [16], but for this Letter we will concentrate on electromagnetic decays between the 4qp high-spin states and their interpretation.

The $M1$ and $E2$ transition operators are defined in Ref. [17]. The calculated transition rates are compared to the experimental values in Fig. 2. In Fig. 2(a), the solid line shows the calculated $B(M1)$ values for transitions within states of the configuration $(N-2)\otimes(\nu g_{9/2})^4$. A standard set of parameters was used: $g_R=Z/A=0.465$, $g_l=0$, $g_s=0.7g_s^{\text{free}}=-2.68$. The calculations reproduce the large staggering which is observed experimentally. We have also investigated the possibility that the quasiparticles are protons. With the same wave functions, the calculated $M1$ transition rates for the $(N-2)\otimes(\pi g_{9/2})^4$ configuration ($g_l=1$,

$g_s = 3.91$) are also seen to reproduce the staggering, as shown by the dot-dashed lines in Fig. 2(a). The effect of mixed proton-neutron configurations has not been investigated yet. Large $M1$ decay matrix elements between states of similar spin, which have been observed in studies of multiparticle state in this mass region, could only be reproduced by mixed proton-neutron configurations, both in the framework of the spherical shell model [2], and in the cranking approach [9]. Therefore, to clarify whether the high-spin states in ^{86}Zr are four-neutron, four-proton, or mixed two-proton–two-neutron configurations coupled to a vibrational core, a determination of the g factors, especially for the 8^+ and 14^+ states, is needed.

The staggering of $B(M1)$ transition rates in our model calculations has a very simple origin. The main component of the wave functions for the even-spin states is the fully aligned state vector $|(g_{9/2})^4 J_F = 12, J_B; J = J_F + J_B\rangle$, where J_F and J_B denote the aligned angular momentum from the fermion and boson parts, while that for the odd-spin states are $|(g_{9/2})^4 J_F = 12, J_B; J = J_F + J_B - 1\rangle$. The doublets of states $(15^+, 16^+)$, $(17^+, 18^+)$, and $(19^+, 20^+)$ have, in leading order, the same structure of the boson part of the wave function. Therefore, for transitions *within* the doublets, the terms contributing to the reduced $M1$ matrix element are large. The wave functions for successive doublets differ by $\Delta J_B = 2$, i.e., the alignment of another d boson along the axis of rotation. Thus, for transitions *between* doublets, the matrix elements corresponding to both the collective and fermion parts of the $M1$ operator vanish in leading order, resulting in the large staggering of $B(M1)$ values.

The calculations also predict the average $B(E2)$ values for these states reasonably well, as can be deduced from Fig. 2(b), where the calculated $B(M1)/B(E2)$ ratios are compared to the experimental values extracted from the $M1/E2$ branching ratios. The large staggering is primarily due to the $B(M1)$ components, while the $B(E2)$ values remain rather constant. The comparison of the absolute $B(E2)$ values depends on the vibrational charge, which has been chosen to reproduce the $B(E2; 2^+ \rightarrow 0^+)$ measured in earlier work [7].

In conclusion, we have studied the transitional nucleus ^{89}Zr to high spins and found a sequence of states whose energy spacings are reminiscent of rotational bands. However, measurements of electromagnetic transition rates between these states show this appearance to be superficial, as the $B(E2)$ values are small and the $B(M1)$ values are staggered and large. These observations are difficult to interpret in terms of rotational models, but are seen to have a natural explanation in an extended IBM-1 model which incorporates two broken boson pairs. The underlying symmetry causing the staggering appears to be a vibrational effect. Measurements of g factors are being planned to disentangle the neutron and proton contributions, and the model needs to be refined in order to include nonidentical quasiparticles, thereby opening up the possibility of understanding the effects of neutron-proton interactions and Pauli blocking at high spins.

We acknowledge many helpful discussions with F. Iachello. This work was supported in part by U.S. DOE Contract No. DE-FG02-91ER-40609 and the Alexander-von-Humboldt Foundation.

(a)Permanent address: Prirodoslovno-matematicki Fakultet, University of Zagreb, 41000 Zagreb, Republic of Croatia, Yugoslavia.

(b)Present address: Department of Physics, University of Tennessee, Knoxville, TN 37996.

[1] C. J. Lister *et al.*, Phys. Rev. Lett. **59**, 1270 (1987).

[2] E. K. Warburton *et al.*, Phys. Rev. C **31**, 1184 (1985).

[3] H. G. Price *et al.*, Phys. Rev. Lett. **51**, 1842 (1983).

[4] J. Hattula *et al.*, Phys. Rev. C **28**, 1860 (1983).

[5] E. K. Warburton *et al.*, Phys. Rev. C **31**, 1211 (1985).

[6] L. Lühmann, thesis, University of Göttingen, 1985 (unpublished); J. Heese, thesis, University of Göttingen, 1989 (unpublished).

[7] M. Avrigeanu *et al.*, J. Phys. G **4**, 261 (1978).

[8] P. M. Endt, At. Data Nucl. Data Tables **23**, 547 (1979).

[9] G. Winter, in Proceedings of the International Conference on High Spin Physics and Gamma-Soft Nuclei, Pittsburgh, 1990 (to be published); L. Funke *et al.*, Phys. Lett. **120B**, 301 (1983).

[10] I. Hamamoto, in *Proceedings of the First Lanzhou Summer School, Lanzhou* (Springer-Verlag, Berlin, 1990); (private communication).

[11] F. Iachello and D. Vretenar, Phys. Rev. C **43**, R945 (1991).

[12] D. Vretenar *et al.*, Phys. Rev. C **42**, 993 (1990).

[13] A. Arima and F. Iachello, Ann. Phys. (N.Y.) **99**, 253 (1976); **111**, 201 (1978); **123**, 468 (1979).

[14] A. I. Kucharska *et al.*, J. Phys. G **15**, 1039 (1989).

[15] L. S. Kisslinger and R. A. Sorensen, Rev. Mod. Phys. **35**, 853 (1963).

[16] P. Chowdhury *et al.* (to be published).

[17] D. Vretenar *et al.*, Phys. Rev. C **44**, 223 (1991).